Recent upgrades to the calibration system of the CMS HCAL

Steffie Ann Thayil[1,*] and *German* Martinez[2] on behalf of the CMS Collaboration

[1]Rutgers University, Piscataway, New Jersey, USA
[2]Florida State University, Tallahassee, Florida, USA

Abstract. The irradiation of the CMS Hadron Calorimeter (HCAL) subdetectors results in decreased signal output from the active materials as well as increased noise in the photodetectors used to read out the system. The HCAL has a dedicated calibration system used to monitor and correct for these effects and to help synchronise the timing of the subdetectors. The calibration system is described with a focus on the upgrades to the laser system, which has undergone significant changes since the end of Run 2 of the LHC in 2018. A new solid state laser has been installed and commissioned, and the optical setup for light distribution has been simplified. An upgrade to the laser trigger board has reduced the laser trigger jitter by an order of magnitude. A new system has also been developed to fire the laser, based on existing HCAL electronics. Future improvements to the system are also presented, including ongoing work on extending the system to include remote monitoring capabilities.

1 Introduction

The Hadron Calorimeter (HCAL) of the CMS experiment is designed to measure the energy and direction of jets and missing transverse energy in collisions at the LHC [1]. The barrel (HB) and endcap (HE) regions of the HCAL are composed of layers of brass absorber plates interleaved with plastic scintillator tiles. The barrel is augmented by an additional layer of scintillators in the outer region beyond the CMS magnet (HO). These subdetectors use wavelength-shifting fibers to carry light from the scintillators to silicon photomultipliers (SiPMs) present on the detector. The HCAL also comprises a Cherenkov detector in the forward region (HF) made of steel absorber with quartz fibers read out by photomultiplier tubes (PMTs).

Figure 1 shows a schematic of the HCAL. Each subdetector is read out by on-detector readout boxes (RBXs) segmented in ϕ. The readout is also segmented in η, and layers belonging to a given η segment are grouped into logical units called megatiles. The Phase 1 HCAL upgrade further introduced depth segmentation in the readout of HB and HE.

All parts of the detector suffer radiation damage with increasing integrated luminosity, seen as decreased signal output from the scintillator tiles and quartz fibers, as well as increased noise and dark current in the SiPMs and PMTs. Some of this damage is temporary and recovers when the beam is turned off. The energy measurements of the detector are therefore dependent on the amount of irradiation and the response must be corrected accordingly.

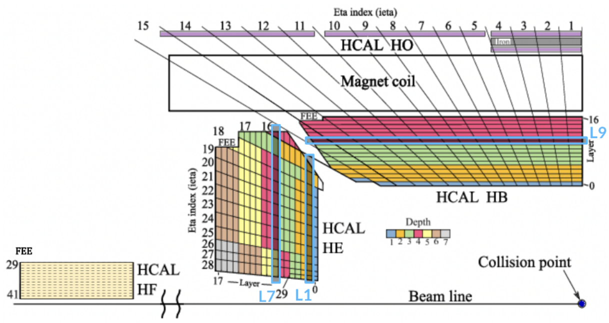

Figure 1. Schematic of the HCAL subdetectors and their readout segmentation as of the start of LHC Run 3. HB and HE have 17 and 18 layers of scintillators respectively. Layer 9 in HB and Layers 1 and 7 in HE, marked in blue, are equipped with quartz fibers used to send light from the laser system directly to the scintillators in these layers. The η segmentation in the readout is shown using iη indices. 'FEE' labels mark the positions of the readout boxes.

2 HCAL calibration system

The HCAL employs a dedicated calibration system to monitor and correct for the effects of radiation exposure and to help synchronize the timing of its subdetectors. It includes the laser system for regular response monitoring, with a separate system implemented for HF since the end of LHC Run 2; calibration units in each front-end readout box for localized LED light distribution; and a ^{60}Co source used during long shutdown periods for comprehensive measurements of radiation damage in the HB and HE scintillators.

The HCAL laser system is a central element of this calibration framework. A laser located in the CMS underground service cavern is used to transmit light via quartz

*e-mail: steffie.ann.thayil@cern.ch

fibers to the detector during breaks in beamtime, approximately once per day. The laser signal can be sent to the photodetectors (SiPMs and PMTs) in each subdetector and to specific scintillator layers within HB (layer 9) and HE (layers 1 and 7).

For radiation damage studies, the response to the calibrated laser light signal is compared against baseline measurements taken at the start of the year. Radiation-induced darkening of the active materials leads to a reduction in the amount of light detected by the photodetectors, while annealing processes result in an increase [2]. Measurements of the strength of this signal are used to derive correction factors for the energy response as a function of radiation dose and recovery time.

The laser can also be used to study changes in the behavior of the photodetectors in response to radiation. Additionally, laser data are useful for identifying missing channels, broken fibers and timing discrepancies.

While the laser system was previously also used to measure radiation damage in the quartz fibers of HF, starting from the end of Run 2, a dedicated system [3] has been employed for this subdetector for reasons described in Sect. 2.1.

The calibration units (CUs) are another important part of the system. The CU in each front-end readout box in the HCAL subdetectors is responsible for receiving and distributing light from the laser. Each CU also has two in situ LEDs that send light to all the photodetectors in that RBX, as well as a small scintillator crystal and PIN diodes to monitor the laser and LED signals.

The final component is the ^{60}Co sourcing system. During long shutdowns, a ^{60}Co source is used with dedicated 'sourcing channels' to measure radiation damage in all the HB and HE scintillators [4]. This offers the distinct advantage of being able to measure the effect of radiation in every individual HB and HE scintillator tile, as opposed to just the three layers accessible to the laser system. However, these measurements can only be taken when the CMS detector is open, requiring an extended period without beam.

Figure 2 shows a block diagram of the HCAL calibration infrastructure and the corresponding run types.

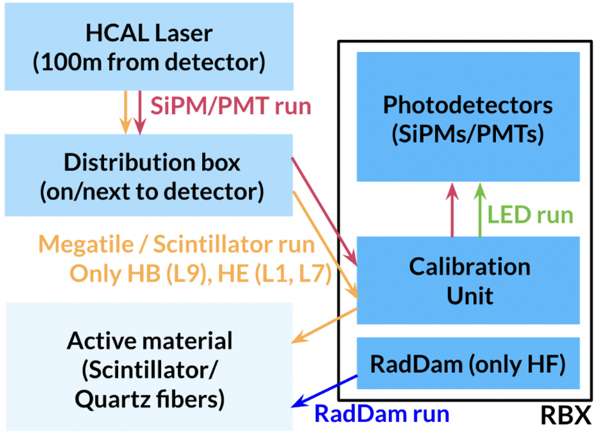

Figure 2. Block diagram of the HCAL calibration infrastructure (sourcing channels not shown). The four types of calibration runs which use the calibration infrastructure are also shown. In addition to these, the baseline response of the detector is monitored by regularly taking 'pedestal runs' to read out the detector with no signal present.

2.1 Motivation for upgrades

Before Run 3, the HCAL laser system used an excimer gas laser, which had certain drawbacks. The gas in the laser would gradually deplete, resulting in a decrease in the laser's power output by ~15% every day. The laser beam spot was also relatively large at ~5 mm. To handle these limitations, a complex optical setup was required, using two rotating variable filter wheels to maintain constant incident laser power on the fibers and a collimator to reduce the size of the beam spot. This setup resulted in substantial inefficiencies in the transmission of light to the detector. The continuous changes in the laser signal strength necessitated regular calibration between LHC fills, and the frequent gas bottle replacements presented a logistical challenge. Moreover, the laser would very occasionally fire without a trigger. The possibility of this happening during a data-taking period meant that the laser could not be used in the abort gap calibration sequence, which are calibration events taken during LHC fills in a small periodic gap between collisions.

In addition to the aforementioned issues, the HF subdetector faced some additional challenges. As a Cherenkov detector, HF is sensitive to blue light instead of UV light as in the rest of HCAL. In the old system, the UV signal from the laser was passed through wavelength-shifting crystals to supply this blue light. However, these crystals degraded quickly in the high radiation environment of the HF. Moreover, the HF readout expects most of the signal to be contained within 25 ns. The crystals used to shift the wavelength of the laser signal also resulted in a broadening of the pulse, necessitating precise timing and a narrower input laser pulse for optimal performance in HF. For these reasons, a dedicated radiation damage monitoring system was developed for HF, modeled after the HF calibration unit and utilizing 450 nm laser diodes mounted on HF readout cards [3].

Finally, the introduction of new CUs was tied to the HCAL Phase 1 upgrade, which saw a complete overhaul of the HCAL photodetectors and front-end electronics. The HB RBXs were replaced in the long shutdown following LHC Run 2 as the last step of this upgrade, following earlier replacements in HO, HF and HE. As was the case for the other subdetectors, new HB CUs were prepared to interface with the new electronics.

3 Laser system upgrade for LHC Run 3

In the long shutdown before Run 3, the laser was upgraded to a Photonics DP20 solid state laser, which is operated in UV at a wavelength of 351 nm. The laser has an energy rating of 4 mJ / pulse which is comparable to the previous laser. However, it has a much more consistent output and a smaller beam spot of ~1 mm, which has allowed for a

https://doi.org/10.1051/epjconf/202532000042

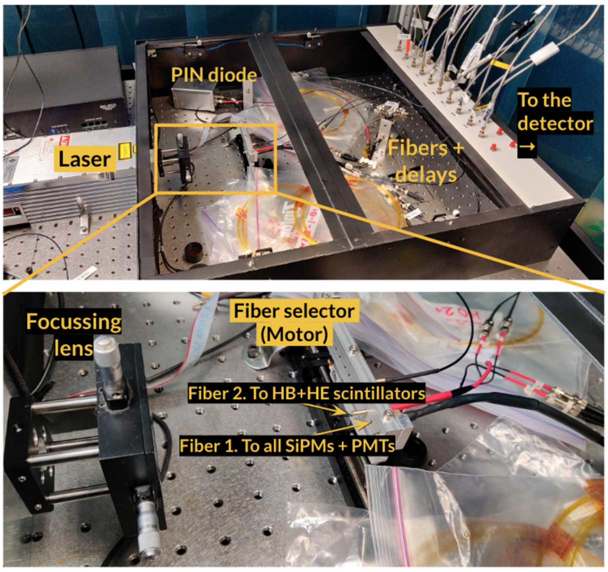

Figure 3. Laser room optical setup (top), zoomed in on lens assembly and fiber selector (bottom)

greatly simplified optical setup. A single convex lens with a focal length of 5 cm is placed at the output of the laser and used to focus the beam into one of two quartz fibers. A linear motor stage is used to change the fiber positioned in front of the beam. The stage is controlled by a National Aperture MC-5CD motion controller. The laser beam and optical setup are contained in a light-tight box with removable covers, installed on an optical breadboard as seen in figure 3 (with the covers removed). The setup is located in the HCAL laser room in the CMS service cavern.

The fibers inside the laser box are connected to outputs on the right side of the box, from where 19 quartz fibers in stainless steel conduits carry the laser light into distribution boxes in the experimental cavern. Out of the 19 fibers, 12 distribute light to the photodetectors, 4 send light to the HB and HE scintillator layers and the last 3 are spares. The fibers are of differing lengths depending on the distance from the laser room to the relevant distribution box. Finally, quartz fibers from the distribution boxes fan out the laser signal to the CUs and from there to their ultimate destinations of either SiPMs, PMTs or scintillator tiles.

Within the laser box, the first fiber (marked as 'Fiber 1' in figure 3) is used to send light to all the SiPMs and PMTs in the four HCAL subdetectors. The fiber is a 1-to-8 splitter with seven 250 μm fibers used to carry the laser signal to the detector and one 125 μm monitoring fiber. Six of the 250 μm fibers are connected via delays to the outputs of the laser box correspondint to the positive and negative halves of HB, HE and HF. The seventh 250 μm fiber goes to a 1-to-6 splitter with one fiber for each half of HO0, HO1 and HO2. Each fiber is connected to a loop of quartz fiber of a different length, used to balance the aforementioned differences in the lengths of the fibers from the service to the experimental cavern. This ensures that all 12 targets have the same total path length for the laser light.

The final 125 μm monitoring fiber from Fiber 1 is connected to a box with a wavelength shifting crystal and a PIN diode whose output is fed to an oscilloscope in the laser room. When the laser box is closed, the oscilloscope can be used by an operator in the laser room to monitor the laser signal in real time.

The second fiber on the linear motor stage ('Fiber 2') is a 1-to-4 splitter used to send light to the HB and HE scintillators, with one fiber each going to the laser box outputs for the positive and negative halves of HB and HE. Fibers carry the signal from the laser room to distribution boxes at the detector, from where the signal is split and injected into each scintillator in layer 9 in HB and layers 1 and 7 in HE, as well as a PIN diode in each CU.

The laser room setup also includes a Coherent energy probe which can be placed in front of the laser beam to measure the energy and the linearity of the response of the internal laser power attenuator.

The new laser system required the development of a set of software tools to simplify operation. Remote communication over Ethernet is possible with both the laser, using a DeviceMaster serial gateway, and the motor controller. A new laser server was developed to handle communication with the laser and fiber selector, respond to commands sent by DCS and DAQ and implement automatic system recovery. A new laser DCS panel was also created to reflect changes to the system.

3.1 Results from the new laser

The laser system was put into operation at the start of LHC Run 3 and successfully took data in its first year. Figure 4 shows some results obtained using the new system. The effects of radiation damage in HE were studied using laser megatile runs to determine the change in the strength of the laser signal over the course of LHC data taking in 2022. The observed trends were used to derive radiation dose dependant corrections to the HE gains. As expected, as the scintillators darken with exposure to radiation, a decrease in the laser signal is seen with increasing integrated luminosity. The effect is more pronounced in parts of the detector that are closer to the beam. The effect of annealing can also be seen as a recovery in laser signal strength over the course of an extended pause in beamtime.

4 New HCAL laser trigger

The laser system was operated successfully in 2022 and offered significant improvements over previous versions. However, it still had some limitations and room for further development.

The new laser was fired using a differential trigger signal supplied by an external board. However, this board behaved quite erratically when powered on, generating spurious triggers at an extremely high rate until it was configured. The laser has a maximum triggering frequency of 100 Hz, requiring the implementation of a safety feature to limit the rate of triggers passed on to the laser, as well a 'safe mode' which closes the laser shutter and turns off the

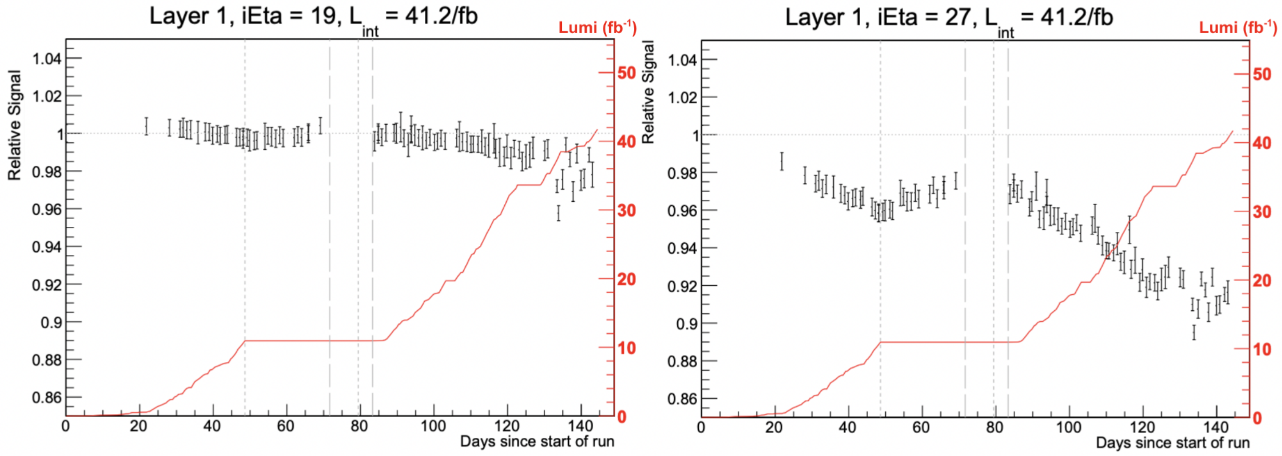

Figure 4. A study of radiation damage in HE Layer 1 in 2022 at iEta=19 (left) and iEta=27 (right), using laser data and corresponding to the 41.2 fb^{-1} of data collected by CMS in 2022. The laser signal is normalised to the signal value in Layer 7 and iEta=±17 in the first run of the year. Higher radiation damage (corresponding to a lower relative signal) is expected in Layer 1 than in Layer 7 because of its proximity to the collision point. Higher radiation damage is also expected at higher values of η (or equivalently, iEta). The plot on the right also shows the recovery in the signal response during the pause in beamtime from day 49-84.

laser diode to prevent accidentally sending unwanted laser pulses into the system.

A more serious issue was that, when powered up, the trigger board had a 50% chance of switching the polarity of the trigger signals sent to the laser. Any such switch caused the laser to fire out of sync with the data acquisition system, resulting in no laser signal being recorded with no immediate way to detect the problem until the data were reviewed. One such incident resulted in a substantial loss of laser data in 2023.

The laser triggering system also operated with a jitter of approximately 10 ns relative to the LHC clock. This was caused by the response of the laser to the external trigger signal. The laser would begin to charge upon receiving a trigger pulse, which was synchronized to the 40 MHz LHC clock. This took ~ 580 µs, after which the laser would start to fire on its internal 100 MHz clock. The laser manufacturer recently developed a modification to the laser, allowing it to accept two external TTL triggers: one to start charging and a second trigger 600 µs later to start firing the laser. Since both these triggers could be aligned with the LHC clock, the implementation of this scheme would allow a great reduction in the jitter.

The laser system also lacked remote monitoring capabilities, since the use of the oscilloscope requires the presence of an operator in the laser room to monitor the signal.

A novel solution was developed to replace the problematic trigger board, supply the two triggers required by the low jitter system and provide remote monitoring at the same time. A spare HB CU has been repurposed for the task, with its two LED driver circuits providing the TTL triggers. Furthermore, a PIN diode in the CU will be used to read out a laser monitoring fiber, employing the same readout scheme as the rest of HB.

Proof-of principle tests were performed using a single LED channel to successfully fire the unmodified laser. The laser was then sent to the manufacturer for the installation of the hardware modification and has recently been returned with the new dual-input trigger card. The full triggering system system is currently being commissioned and is expected to be in operation before the end of the 2024 LHC run.

5 Conclusions

The HCAL calibration system has seen numerous impactful improvements since the end of LHC Run 2. The upgraded laser system has been successfully operated and proven effective for radiation damage studies.

A new trigger system was developed for the laser and is currently being commissioned. This will be followed by the development and commissioning of a remote monitoring system for the laser signal.

References

[1] A. Hayrapetyan et al., Development of the CMS detector for the CERN LHC Run 3. JINST **19** P05064 (2024).

[2] A.M. Sirunyan et al., Measurements with silicon photomultipliers of dose-rate effects in the radiation damage of plastic scintillator tiles in the CMS hadron endcap calorimeter. JINST **15** P06009 (2020).

[3] B. Bilki and Y. Onel, Design, Construction and Commissioning of the Upgrade Radiation Damage Monitoring System of the CMS Hadron Forward Calorimeters. Proceedings, 2018 IEEE Nuclear Science Symposium and Medical Imaging Conference (NSS/MIC 2018).

[4] S. Chatrchyan et al., Radioactive source calibration test of the CMS Hadron Endcap Calorimeter test wedge with Phase I upgrade electronics. JINST **12** P12034 (2017).